Comparison of Different Supramolecular Architectures for Oligonucleotide Biosensing

Mònica Mir,*,† Marta Álvarez,† Omar Azzaroni,*,‡ and Wolfgang Knoll†

Max-Planck-Institut für Polymerforschung, Ackermannweg 10, 55128 Mainz, Germany, and Instituto de Investigaciones Fisicoquímicas Teóricas y Aplicadas (INIFTA), CONICET, Universidad Nacional de La Plata, CC. 16 Suc.4, (1900) La Plata, Argentina

Received July 12, 2008. Revised Manuscript Received September 5, 2008

This work describes a comparative study between two biosensing platforms that are commonly used to immobilize capture probes. These platforms refer to thiolated and biotinylated oligonucleotide strands chemisorbed on Au surfaces (DNA SAM) and bioconjugated on streptavidin (SA) monolayers (SA SAM), respectively. Both interfacial architectures were studied using surface acoustic wave (SAW) devices and surface plasmon spectroscopy (SPR). Our studies indicated that DNA SAM platforms enable higher densities of surface-confined oligonucleotide probes. However, their hybridization efficiency is lower when compared to that obtained in SA SAM platforms, thus impacting on a lower detection limit, 5 nM. Furthermore, binding of SA molecules to the biotinylated targets, in an attempt to enhance the signal in both platforms, revealed striking differences between both architectures. The SA underlayer used in the SA SAM configuration confers nonfouling characteristics to the interfacial assembly, thus precluding the nonspecific binding of SA onto the surface. The antifouling behavior of the SA DNA platform is an important feature to be considered in the amplification of hybridization events through the bioconjugation of biotinylated targets with streptavidin-based tags.

Introduction

DNA sensors represent a key tool in molecular biology and biotechnology with growing relevance during recent years. The results of the human genome project further increased the possible applications of DNA sensing including diagnostics of genetic diseases, detection of infectious agents, drug screening, environmental monitoring or forensic science, just to name a few examples.[1−5]

The fabrication of DNA sensors involves the immobilization of a capture probe, which is a single-stranded DNA (ssDNA) complementary to the target oligonucleotide. The same surface architecture is also valid to probe chemical variations of DNA such as peptide nucleic acid (PNA)[6] or locked nucleic acid (LNA).[7] There are different methods to immobilize the capture probes on the biosensor surface. The most straightforward one is the direct adsorption of the DNA on the surface. Materials reported for this type of immobilization include nitrocellulose,[8] nylon membranes,[9] polystyrene, and metal[10] and carbonaceous[11] surfaces. Adsorption is the simplest method to immobilize DNA, because it does not require any other reagent or any special modification of the nucleic acids. However, the main drawback of this method is the poor hybridization efficiency and the inherent instability of the nucleic acid physisorbed on the surface.

ssDNA can also be retained in meshes[12] or composites[13] that have been previously immobilized on a solid support. Meshes are characterized by their large area of adsorption, which increases the amount of oligonucleotide strands attached to their surface, thus increasing the sensitivity of the system. However, the lack of oligonucleotide orientation sensitively decreases the accessibility to the captured molecules. The details of the oligonucleotide orientation at surfaces have been recently addressed by Goldberg and co-workers. These researchers using spectral self-interference fluorescence microscopy have estimated the shape of coiled single-stranded DNA, the average tilt of double-stranded DNA of different lengths, and the amount of hybridization.[14]

A more robust immobilization can be achieved via chemical linkage between functional groups confined on the surface and reactive groups of the DNA, which should not affect the hybridization event.[15] A most widespread immobilization method for DNA sensing is via a self-assembled monolayer (SAM) of thiolated ssDNA (HS-ssDNA)[16] chemisorbed on a

* To whom correspondence should be addressed. E-mail: azzaroni@inifta.unlp.edu.ar (O.A.); mir@mpip-mainz.mpg.de (M.M.).

† Max-Planck-Institut für Polymerforschung.

‡ Universidad Nacional de La Plata.

(1) White, D. C.; Gouffon, J. S.; Peacock, A. D.; Geyer, R.; Biernacki, A.; Davis, G. A.; Pryor, M.; Tabacco, M. B.; Sublette, K. L. *Environ. Forensics* **2003**, *4*, 63.

(2) Takacs, K.; Nemedi, E.; Marta, D.; Gelencser, T.; Kovacs, E. T. *Acta Aliment.* **2007**, *36*, 195.

(3) Waggoner, P. S.; Craighead, H. G. *Lab Chip* **2007**, *7*, 1238.

(4) Patolsky, F.; Zheng, G.; Lieber, C. M. *Nanomedicine* **2006**, *1*, 51.

(5) Rusling, J. F.; Hvastkovs, E. G.; Schenkman, J. B. *Curr. Opin. Drug Discovery Dev.* **2007**, *10*, 67.

(6) (a) Liu, J. Y.; Tiefenauer, L.; Tian, S. J.; Nielsen, P. E.; Knoll, W. *Anal. Chem.* **2006**, *78*, 470. (b) Mir, M.; Álvarez, M.; Azzaroni, O.; Tiefenauer, L.; Knoll, W. *Anal. Chem.* **2008**, *80*, 6554–6559.

(7) Liu, J. P.; Drungowski, M.; Nyarsik, L.; Schwartz, R.; Lehrach, H.; Herwig, R.; Janitz, M. *Comb. Chem.* **2007**, *10*, 269.

(8) Wang, J.; Cai, X.; Rivas, G.; Shiraishi, H.; Farias, P. A. M.; Dontha, N. *Anal. Chem.* **1996**, *68*, 2629.

(9) Wang, J.; Cai, X.; Fernandes, J. R.; Grant, D. H.; Ozsoz, M. *Anal. Chem.* **1997**, *69*, 4056.

(10) Pang, D. W.; Abruña, H. D. *Anal. Chem.* **1998**, *70*, 3162.

(11) Marrazza, G.; Chianella, I.; Mascini, M. *Biosens. Bioelectron* **1999**, *14*, 43.

(12) Li, D. P.; Frey, M. W.; Baeumner, A. J. *J. Membr. Sci.* **2006**, *279*, 354.

(13) Millan, K. M.; Saraullo, A.; Mikkelsen, S. R. *Anal. Chem.* **1994**, *66*, 2943.

(14) Moiseev, L.; Ünlü, M. S.; Swan, A. K.; Goldberg, B. B.; Cantor, C. R. *Proc. Natl. Acad. Sci. U.S.A.* **2006**, *103*, 2623–2628.

(15) Mikkelsen, S. K. *Electroanalysis* **1996**, *8*, 15.

(16) (a) Levicky, R.; Herne, T. M.; Tarlov, M. J.; Satija, S. K. *J. Am. Chem. Soc.* **1998**, *120*, 9787. (b) Petrovykh, D. Y.; Kimura-Suda, H.; Whitman, L. J.; Tarlov, M. J. *J. Am. Chem. Soc.* **2003**, *125*, 5219–5226. (c) Steel, A. B.; Levicky, R. L.; Herne, T. M.; Tarlov, M. J. *Biophys. J.* **2000**, *79*, 975–981. (d) Herne, T. M.; Tarlov, M. J. *J. Am. Chem. Soc.* **1997**, *119*, 8916–8920. (e) Kimura-Suda, H.; Petrovykh, D. Y.; Tarlov, M. J.; Whitman, L. J. *J. Am. Chem. Soc.* **2003**, *125*, 9014–9015.

10.1021/la802228e CCC: $40.75
Published on Web 10/24/2008

Scheme 1. Chemical Structure of the Biotinylated Thiol Used for the Preparation of the SA SAM

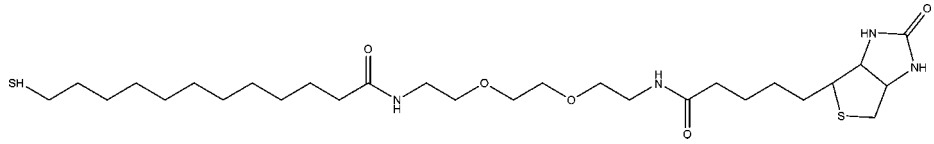

gold surface. The strong interaction between the thiol group and the gold surface results in a robust linkage similar to a covalent bond.[17]

On the other hand, the use of streptavidin (SA) monolayers is receiving increasing attention for the immobilization of biotinylated ssDNA.[18,19] SA is a 60 kDa protein purified from the bacterium *Streptomyces avidinii* presenting extremely high and very specific interactions[20] with biotin ($K = 10^{15}$ L mol^{-1}). The linkage is very strong and is affected only under extreme conditions. This protein has four binding sites for biotin located on two opposite sides of the tetrameric protein. It can thus be used to link two different functions in the new molecular complex. This means that the protein has unique properties as a building block for the binding of a second layer of biotinylated molecules.

The differences between both interfacial architectures would probably have an impact on their probe densities and hybridization efficiencies, thus influencing their performance and characteristics to a large extent. For example, Lee et al. demonstrated that the chemisorption of mercaptoundecanol on a HS-ssDNA-modified Au surface leads to the reorientation of the oligomers into a more upright position followed by the displacement of oligonucleotides from the surface.[21] Moreover, incorporating functional tags into the DNA assembly to amplify the hybridization readout signal is gaining increasing interest within the research community. A most common procedure is based on conjugating streptavidin-based labels such as fluorescent probes, enzymes, nanoparticles, or electroactive materials to biotinylated targets hybrized on the sensor surface.[22] However, little is known about the interaction between streptavidin and biotinylated double-stranded (ds) DNA confined in both interfacial architectures. As a consequence, a detailed study comparing both platforms is mandatory in order to achieve a deeper understanding of the molecular design of biosensing interfaces.

In this work, we performed a comparative study on the biosensing characteristics of thiolated oligonucleotide strands chemisorbed on Au surfaces and their biotinylated analogues bioconjugated on streptavidin monolayers. Our results indicate that the nature of the supramolecular architecture strongly influences the hybridization efficiency and has an impact on the detection limit. Binding studies of SA bioconjugated to biotin-terminated hybridized DNA strands then revealed that the appearance of nonspecific adsorption can be substantially suppressed in the presence of SA as an anchoring layer.

Materials and Methods

Materials and Equipment. The oligonucleotide sequences an 18-mer thiol labeled capture probe (SH−C_6−5′-TTTTGTACAT-CACAACTA-3′), an 18-mer biotinylated capture probe (biotin−5′-TTTTGTACATCACAACTA-3′), and a 15-mer biotinylated target (biotin−5′-TAGTTGTGATGTACA-3′) involved in this work were purchased from MWG Biotech AG. All stock oligonucleotide solutions were prepared at 100 μM with Milli-Q water and stored at −20 °C.

Streptavidin (SA), mercaptoundecanol, 2-mercaptoethanol, phosphate buffered saline (PBS), and polyethylene glycol sorbitan monolaurate (Tween 20) were purchased from Sigma. Biotin terminated thiol was from Roche Diagnostics (Scheme 1).

Mixed Self-Assembled Monolayers of ssDNA (DNA SAM). A mixed SAM of 2-mercaptoethanol and thiolated ssDNA was used to obtain the ssDNA layer on the gold surface. First, the gold substrates were incubated during 2 h in a 1 μM solution of the thiolated capture probe (in 1 M KH_2PO_4). The ssDNA-modified gold substrates were then incubated during 1 h in 1 mM 2-mercaptoethanol aqueous solution (backfilling step). The backfilling was carried out by the sequential chemisorption of 2-mercaptoethanol after immobilizing the thiolated oligonucleotide strands. This promotes the reorientation of the DNA chains, enabling an optimized conformation for a rapid hybridization process as indicated by previous experiments reported by Arinaga et al.[23] and Castner et al.[21]

The immobilized capture probes were incubated in different solutions of biotinylated oligonucleotide target (in 0.1 M PBS solution, pH 7.4). Bioconjugation of SA to the biotinylated targets to enhance the hybridization signal was accomplished by injecting a 1 μM SA solution (in 0.1 M PBS, pH 7.4) into the SPR or SAW sample chamber. The sensors were washed with 0.1 M PBS solution between individual steps in order to remove all nonspecifically bound proteins

ssDNA Immobilization by Affinity Interactions onto a SA Monolayer (SA SAM). Gold substrates were incubated overnight in an ethanolic solution constituted of a 1:9 mixture of biotin-terminated thiol (0.05 mM) and 11-mercapto-1-undecanol (0.45 mM). Afterward, the surface was rinsed with ethanol and dried with N_2. This mixture gives the optimum coverage of biotin centers to achieve maximum binding of SA. These particular conditions are based on experimental evidence reported by Spinke et al.[24] and corroborated by López and co-workers.[25]

Afterward, the biotinylated gold substrates were incubated for 1 h in 1 μM SA (in PBS solution, pH 7.4). The assembly of SA was followed by bioconjugation of the biotinylated capture probes using a 1 μM solution (in 0.1 M PBS, pH 7.4) during 1 h. Finally, the capture probes were hybridized in 1 μM biotinylated targets during 1 h. Careful washing steps were carried out between each layer deposition in order to remove nonspecifically adsorbed molecules.

(17) Dubois, L. H.; Nuzzo, R. G. *Annu. Rev. Phys. Chem.* **1992**, *43*, 437.
(18) (a) Knoll, W.; Liley, M.; Piscevic, D.; Spinke, J.; Tarlov, M. J. *Adv. Biophys.* **1997**, *34*, 231. (b) Su, X.; Wu, Y. J.; Robelek, R.; Knoll, W. *Langmuir* **2005**, *21*, 348–353. (c) Smith, C. L.; Milea, J. S.; Nguyen, G. H. *Top. Curr. Chem.* **2006**, *261*, 63–90. (d) Larsson, C.; Rodahl, M.; Höök, F. *Anal. Chem.* **2003**, *75*, 5080–5087. (e) Ijiro, K.; Ringsdorf, H.; Birch-Hirschfeld, E.; Hoffmann, S.; Schilken, U.; Strube, M. *Langmuir* **1998**, *14*, 2796–2800.
(19) Schott Nexterion (commercially available streptavidin-coated substrates), http://www.us.schott.com/nexterion.
(20) Weber, P. C.; Ohlendorf, D. H.; Wendoloski, J. J.; Salemme, F. R. *Science* **1989**, *243*, 85–88.
(21) Lee, C.-Y.; Gong, P.; Harbers, G. M.; Grainger, D. W.; Castner, D. G.; Gamble, L. J. *Anal. Chem.* **2006**, *78*, 3316–3325.
(22) (a) Kim, N. H.; Baek, T. J.; Park, H. G.; Seong, G. H. *Anal. Sci.* **2007**, *23*, 177–181. (b) Weizmann, Y.; Patolsky, F.; Willner, I. *Analyst* **2001**, *126*, 1502–1504. (c) Willner, I.; Patolsky, F.; Weizmann, Y.; Willner, B. *Talanta* **2002**, *56*, 847–856. (d) Patolsky, F.; Lichtenstein, A.; Willner, I. *Nat. Biotechnol.* **2003**, *19*, 53–257. (e) Patolsky, F.; Lichtenstein, A.; Willner, I. *Chem.—Eur. J.* **2003**, *9*, 1137–1145.
(23) Arinaga, K.; Rant, U.; Tornow, M.; Fujita, S.; Abstreiter, G.; Yokoyama, N. *Langmuir* **2006**, *22*, 5560–5562.
(24) Spinke, J.; Liley, M.; Schmitt, F. J.; Guder, H. J.; Angermaier, L.; Knoll, W. *J. Chem. Phys.* **1993**, *99*, 7012.
(25) Pérez-Luna, V. H.; O'Brien, M. J.; Opperman, K. A.; Hampton, P. D.; López, G. P.; Klumb, L. A.; Stayton, P. S. *J. Am. Chem. Soc.* **1999**, *121*, 6469–6478.

Scheme 2. Simplified Scheme Describing Both Supramolecular Interfacial Architectures Used in This Work: Biotinylated Oligonucleotide Strands Conjugated on a Streptavidin Monolayer (SA SAM) (on the Left) and Thiolated Oligonucleotide Strands Chemisorbed on a Au Surface (DNA SAM) (on the Right); the Different Building Blocks Are Also Indicated

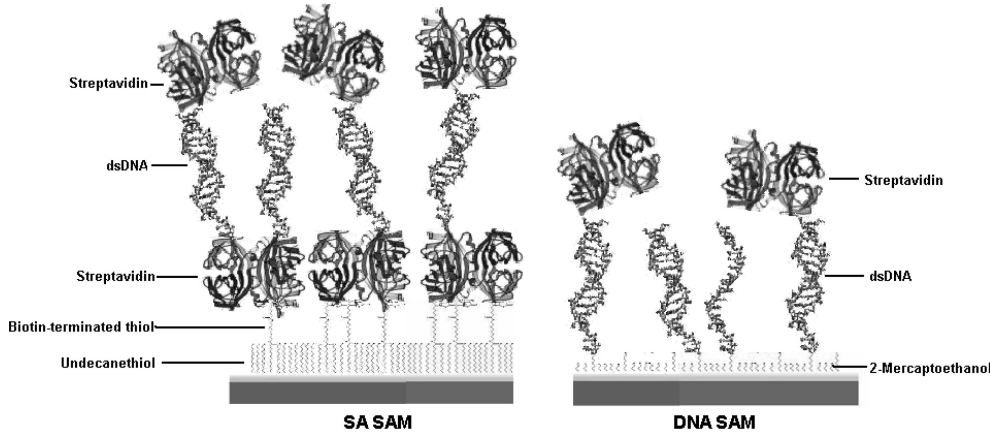

Surface Acoustic Wave (SAW) Sensing. SAW measurements were carried out with an S-sens k5 system from Nanofilm Surface Analysis (Germany). This equipment works with shear waves to ensure low damping of the acoustic waves in an aqueous environment and with Love waves to provide high wave amplitudes at the sensor surface, improving the sensitivity. The sensor chip array consists of five gold sensors with a sensing area of 6.3 mm^2 each. Two interdigitated arrays are placed on each side of the sensor: one transforms the electrical signal into an acoustic wave, and the second array transforms the acoustic wave into an electrical signal. The sensors were cleaned with plasma treatment in a 200G plasma system from Technics Plasma GmbH for 5 min at 300 W under argon atmosphere. All incubations were programmed, and injection was done automatically at a flow rate of 20 μL min^{-1} at 25 °C. The substrates were rinsed by injecting during 5 min 0.1 M PBS buffer at a flow rate of 20 μL min^{-1} at 25 °C. After each experiment, an injection of 5% glycerol solution was required for calibration purposes.[26] The experimental values described in the plots were obtained after averaging four measurements.

Surface Plasmon Spectroscopy (SPR) Measurements. The SPR substrates were BK7 glass slides ($n = 1.5151$, $\lambda = 632.8$ nm) (Menzel-Gläser) coated with 2 nm chromium + 50 nm gold film, which were deposited by evaporation with an Edwards Auto 306 evaporator.

Surface plasmon spectroscopy was performed in the Kretschmann configuration with a custom-made setup.[27] The instrument contains a HeNe laser (Uniphase) operating at $\lambda = 632.8$ nm that passes a chopper (EG&G), an intensity polarizer, and a control polarizer (Glan-Thompson polarizer, Owis) before being reflected off the base of a 90° high index glass prism ($n = 1.8449$) on a two goniometer arrangement (Huber). A photodiode (BPW 34Bsilicon) collects the reflected light. The reflected intensity is monitored as a function of the angle of incidence, which gives the angular reflectivity scans. The SPR angle shifts were converted into mass uptakes using the experimentally determined relationship, Γ (ng mm^{-2}) = $\Delta\theta$ (deg)/0.19. The sensitivity factor was obtained following procedures reported in the literature.[28] During the experiments, samples were injected in the SPR chamber at a flow rate of 100 μL min^{-1} at 25 °C.

In the case of oligonucleotide hybridization, the limit of detection (LOD) was estimated following the guidelines recommended by the International Union of Pure and Applied Chemistry (IUPAC) which defines the LOD as 3 times the signal rms plus the mean background.[29]

Results and Discussion

We compared two different interfacial architectures used for detecting DNA hybridization. These platforms are based on different strategies for anchoring the oligonucleotide probes. Scheme 2 depicts both supramolecular architectures indicating the different building blocks constituting the platform.

To compare the different characteristics of both platforms, we studied the changes in phase signals obtained with the SAW device in two sequential steps: (a) after the hybridization of the surface-confined capture probes with different target concentrations and (b) after the bioconjugation of the biotinylated targets with 1 μM SA (Figure 1).

Hybridization of the capture probe at the high target concentrations (1 μM) yields a higher response in the case of the SA SAM platform (2.6° versus 1.4° in DNA SAM) (Figure 1). This implies that the SA SAM platform is more sensitive, achieving detection limits of 5 nM. Conversely, in the DNA SAM configuration, the lowest target concentration that can be detected above the background signal is 100 nM. In this respect, it is worthwhile to mention that both platforms (SAM DNA and SA DNA) could operate under different kinetic regimes,[30] which would imply that assay completion could have different time windows. Another explanation for the different detection limits could be attributed to nonspecific immobilization of target DNA on the HS-ssDNA-modified surface. In this context, Castner and co-workers introduced the use of HS-ssDNA covalently attached to maleimide-ethylene glycol disulfide monolayers[31] or HS-ssDNA diluted with short thiolated oligo(ethylene glycol).[32]

Once the oligonucleotide targets were hybridized, a further enhancement of the sensor signal was achieved by conjugating the SA to the biotinylated target strands. In this case, SA is acting as a tag for amplifying the readout. Figure 1 shows the response from both systems due to the interaction of SA with

(26) Saha, K.; Bender, F.; Rasmusson, A.; Gizeli, E. *Langmuir* **2003**, *19*, 1304–1311.

(27) Knoll, W. *Annu. Rev. Phys. Chem.* **1998**, *49*, 569.

(28) (a) Yu, F. Ph.D. Thesis, Johannes Gutenberg-Universität, Mainz, Germany, 2004; http://www.mpip-mainz.mpg.de/knoll/publications/thesis/yu_2004.pdf. (b) Stenberg, E.; Persson, B.; Roos, H.; Urbaniczky, C. *J. Colloid Interface Sci.* **1991**, *143*, 513–526.

(29) (a) Thomsen, V.; Schatzlein, Mercuro, D. *Spectroscopy* **2003**, *18*, 112–114. (b) Lau, K. H. A. Ph.D. Thesis, Johannes Gutenberg-Universität, Mainz, Germany, 2008; http://www.mpip-mainz.mpg.de/knoll/publications/thesis.

(30) Caruana, D. J. In *Biosensors: A Practical Approach*; Cooper, J., Cass, T., Eds.; Oxford University Press: New York, 2004; Chapter 2, pp 19−39.

(31) Lee, C.-Y.; Nguyen, P.-C. T.; Grainger, D. W.; Gamble, L. M.; Castner, D. G. *Anal. Chem.* **2007**, *79*, 4390–4400.

(32) Lee, C.-Y.; Gamble, L. J.; Grainger, D. W.; Castner, D. G. *Biointerphases* **2006**, *1*, 82–92.

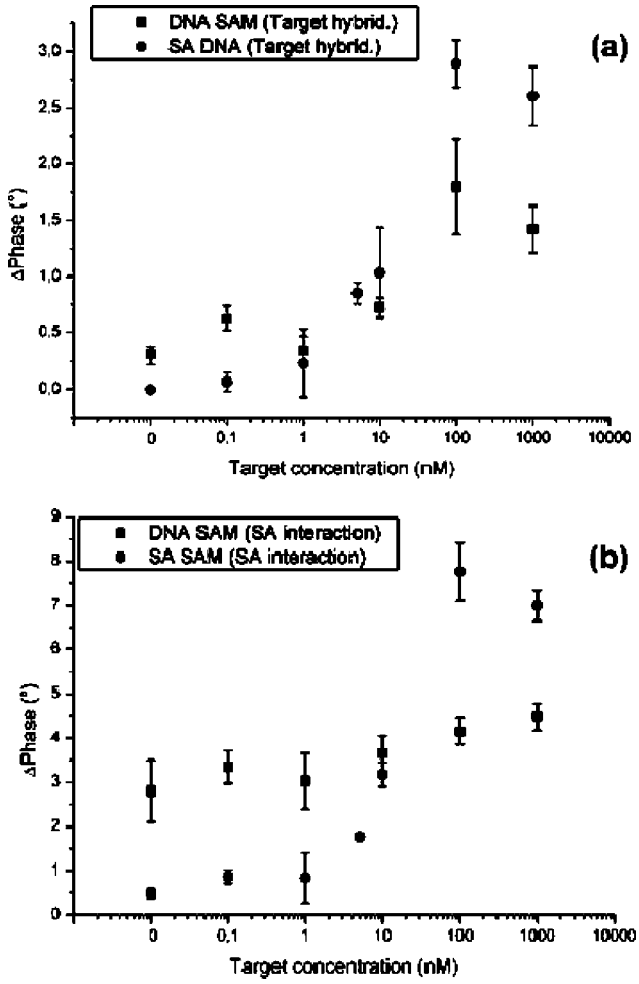

Figure 1. (a) Phase changes obtained in both interfacial architectures after hybridizing the capture probes at different target concentrations. (b) Phase changes recorded after interacting 1 μM SA (in PBS, pH 7.4) with the biotinylated oligonucleotide targets immobilized at different concentrations.

the biotinylated DNA target at different concentrations. The enhancement of the signal due to the interaction of SA with the platforms is clearly seen; however, no improvement of the detection limit in either of the two systems is observed.

Despite these findings, relevant information central to our work can be obtained from these results. From the analysis of phase signal changes at very low target concentrations, it can be observed that significant nonspecific adsorption is affecting the readout of the DNA SAM platform while in the SA SAM architecture this phenomenon is observed to a lesser extent (Figure 1b). For example, at zero target concentration, the DNA SAM configuration showed an increase in the phase signal of roughly 3° while it was virtually 0° for the SA SAM platform (Figure 1b). This is clear evidence that a significant amount of nonspecifically adsorbed SA molecules were retained on the DNA SAM platform after rinsing the sensor surface.

This observation is in agreement with recent results reported by van Oss and co-workers.[33] These authors discussed the macroscopic-scale surface properties of SA and their influence on the nonspecific interactions with biopolymers. SA-coated glass substrates presented highly hydrophilic surface properties and prevented the fouling of biomolecules such as immunoglobulins (IgG) or human serum albumin (HSA).[33] The "hydrophilic repulsion", as described in detail by van Oss, originates from very hydrophilic molecules that attract water molecules more strongly than the free energy of attraction of these molecules or particles for one another, plus the hydrogen-bonding free energy of cohesion between the water molecules, thus resulting in a net nonelectrical double layer repulsion.[34] The hydrophilic repulsion between the SA-coated surface and the IgG or HSA precluded the nonspecific binding to the surface, to which biotinylated molecules can be easily and firmly attached. These results explain our experimental observation indicating that in the SA SAM platform the SA underlayer repels the nonspecifically bound proteins. According to van Oss et al., this antifouling behavior is governed by macroscopic-scale hydrophilic repulsion between the SA-coated surface and the biomolecules. In aqueous solutions, biomacromolecules such as IgG or HSA cannot approach the SA layer closer than 3 nm, which is enough to prevent any nonspecific binding to the interfacial architecture. In our case, the SA underlayer would be responsible for conferring similar properties to the supramolecular assembly, where a strong hydrophilic repulsion would prevent the nonspecific binding of SA from solution.

The different fouling properties of these platforms are an important point to take into account prior to choosing the right platform for biosensing. This choice can be a concern when the amplification of the biorecognition event heavily depends on the specificity of the biotin−streptavidin interaction to accurately introduce a number of functional tags (fluorophores, redox labels, nanoparticles, and others) into the biosensing platform.[22] As a consequence, building an interfacial architecture having suitable recognition sites to bind specific ligands into a nonfouling environment represents a major achievement in the molecular design of biosensing platforms.

To gain a better understanding of the differences in the hybridization efficiency and fouling properties, we studied both platforms with SPR. The immobilization of biomolecules on the sensor surface was detected by measuring the shift of the minimum in the reflectivity versus angle-of-incidence scans, which is proportional to surface coverage. In our calibrated experimental setup, the mass coverage was estimated using a sensitivity factor corresponding to the relationship Γ (ng mm^{-2}) = $\Delta\theta$ (deg)/0.19.[28]

The coverage of thiolated capture probes chemisorbed on the Au surface (DNA SAM platform) resulted in 0.050 pmol mm^{-2} (Figure 2). The hybridization of the capture probe with the biotinylated target resulted in the immobilization of 0.010 pmol mm^{-2} of complementary oligonucleotide, which gives a hybridization efficiency of 20% in the DNA SAM configuration. The hybridization efficiency was calculated by the ratio between hybridized targets and immobilized capture probes. These results are in quite good agreement with recent results reported by Goldberg et al., in which capture probes with a surface density of 0.035 pmol mm^{-2} displayed a hybridization efficiency of 30−50%.[14] It is worth mentioning that other groups also working with thiolated capture probes reported higher surface probe densities, 1.7×10^{13}−4.4×10^{13} probes cm^{-2}, thus achieving hybridization efficiencies in the 8−13% range.[35] The reduced hybridization efficiency at higher probe densities can be explained by electrostatic repulsion between close packed oligonucleotides

(33) van Oss, C. J.; Giese, R. F.; Bronson, P. M.; Docoslis, A.; Edwards, P.; Ruyechan, W. T. *Colloids Surf., B* **2003**, *30*, 25.

(34) van Oss, C. *J. Mol. Recognit.* **2003**, *16*, 177–190.

(35) Gong, P.; Lee, C.-Y.; Gamble, L. J.; Castner, D. G.; Grainger, D. W. *Anal. Chem.* **2006**, *78*, 3326–3334.

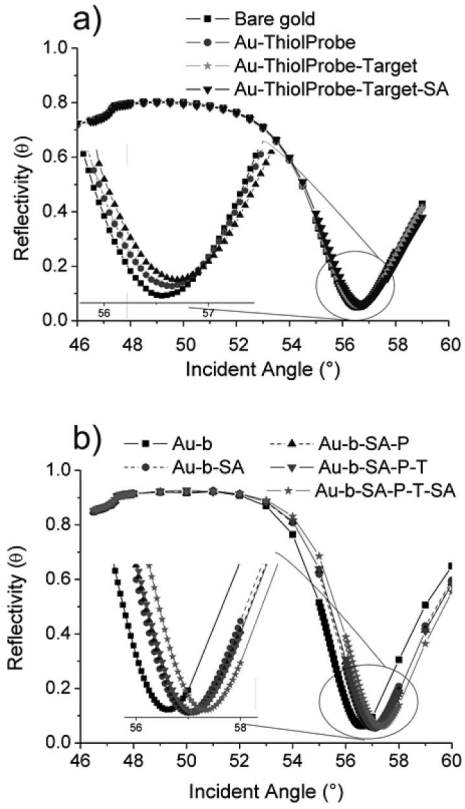

Figure 2. Reflected intensity as a function of the angle-of-incidence scan (θ) describing the supramolecular assembly of the different interfacial architectures: (a) DNA SAM and (b) SA SAM. The insets show the expanded view of the SPR minimum part indicated with gray circles in panels (a) and (b).

and steric hindrance of target DNA. In our case, the subsequent interaction of biotinylated target with SA led to a surface coverage of 0.014 pmol mm^{-2}. The fact that the coverage of SA molecules is higher than the coverage of biotinylated targets corroborates the presence of nonspecific adsorption of SA molecules, as previously detected by SAW. Assuming 100% efficiency for the interaction between SA and the biotinylated targets, these results would indicate that ~40% of the SA molecules are nonspecifically bound to the sensing platform.

The multilayered SA SAM architecture was also studied by SPR and compared to the DNA SAM platform. The surface coverage of the first SA layer was 0.040 pmol mm^{-2}, which is equivalent to ~230 ng cm^{-2}. This value is in complete agreement with recent results reported by Nelson et al.[36] and Jung et al.[37] working with mutant and wild-type streptavidins on similar biotinylated SAMs who estimated 230 ng cm^{-2} for SA coverage. The coverage of biotinylated capture probes then turned out to be 0.034 pmol mm^{-2}. The resulting SA/biotinylated capture probe ratio was 1:0.85. Even if it is assumed the SA exposes two biotin binding sites to the solution, the SPR results indicate that nearly each SA is conjugated to one biotinylated target. This has been attributed to a combination of electrostatic repulsion and steric hindrance of the oligonucleotide strands that precludes the coordination of the second binding site.[38,39] The coverage of the capture probes on the SA SAM configuration was lower than that estimated in the DNA SAM platform; however, the SA SAM platform achieved a higher hybridization efficiency, ~90%. The high hybridization efficiency of the SA SAM platform may be surprising if we consider that the hybridization efficiency is highly dependent on the capture probe coverage. Notwithstanding this observation, in the SA SAM platform, like in other platforms,[40] a lower capture probe density yielded a higher hybridization efficiency. The SA molecules act as building blocks in the construction of organized supramolecular architectures[41] capable of forming a monomolecular capture probe layer. This surface architecture provides a sufficient binding area and allows optimum anchoring of the capture probe in order to avoid steric hindrance and minimizing the repulsion between negatively charged strands. These characteristics facilitate the hybridization of target oligonucleotides from solution with the surface-confined capture probes. Conversely, the target molecules encounter more difficulties to hybridize in the DNA SAM platform due to high density of the capture probes. In a similar fashion, the higher amount of target oligonucleotides hybridized on the SA SAM platform (0.031 pmol mm^{-2}) in comparison to the DNA SAM architecture (0.010 pmol mm^{-2}) explains the higher phase increase detected by the SAW device.

The SA layer conjugated to the biotinylated dsDNA, that is, the topmost SA layer, in the SA SAM architecture led to a SA coverage of 0.031 pmol mm^{-2}, thus resulting in a conjugation efficiency to the biotinylated target of ~100%. This value has been obtained considering the background signal (close to zero) obtained in the control experiments without target oligonucleotides.

Conclusions

In this work, we carried out a comparative study between two biosensing platforms constituted of thiolated and biotinylated oligonucleotide strands chemisorbed on Au surfaces (DNA SAM) and bioconjugated on SA monolayers (SA SAM), respectively. Our studies indicated that the interfacial architecture provided by the DNA SAM platform enables higher densities of oligonucleotide probes confined on the sensor surface. However, the higher probe density promotes lower hybridization efficiencies in comparison to those obtained in SA SAM architectures. The differences in interfacial architecture also have an impact on the detection limits. SAW results indicated that the SA SAM achieves a lower detection limit (~5 nM) when compared to the DNA SAM (~100 nM).

Signal enhancement through the binding of SA molecules to the biotinylated targets displayed interesting differences between both supramolecular architectures. Our results derived from SAW and SPR meaurements indicate that the SA monolayer used in the SA SAM architecture confers significant antifouling characteristics to the biosensing platform. In other words, the SA underlayer helps to control and minimize the nonspecific binding of SA molecules from solution. This is a new outstanding feature of the SA SAM platform with strong implications on the widespread use of streptavidin-based tags to amplify hybridization events using different readout systems. We consider that these results promote a better understanding of the molecular design

(36) Nelson, K. E.; Gamble, L.; Jung, L. S.; Boeckl, M. S.; Naeemi, E.; Gollegde, S. L.; Sasaki, T.; Castner, D. G.; Campbell, C. T.; Stayton, P. S. *Langmuir* **2001**, *17*, 2807–2816.
(37) Jung, L. S.; Nelson, K. E.; Stayton, P. S.; Campbell, C. T. *Langmuir* **2000**, *16*, 9421–9432.
(38) Yang, N.; Su, X. D.; Tjong, V.; Knoll, W. *Biosens. Bioelectron.* **2007**, *22*, 2700.
(39) Larsson, C.; Rodahl, M.; Hook, F. *Anal. Chem.* **2003**, *75*, 5080.
(40) Peterson, A. W.; Heaton, R. J.; Georgiadis, R. M. *Nucleic Acids Res.* **2001**, *29*, 5163.
(41) Azzaroni, O.; Mir, M.; Knoll, W. *J. Phys. Chem. B* **2007**, *111*, 13499–13503.

of biosensing platforms as well as they provide a route for the construction of biosensing platforms incorporating nonfouling properties. We envision that these platforms resisting the nonspecific binding of SA from solution will be of great benefit for those interested on using streptavidin-based tags to amplify biosensing readouts, as they can reduce significantly the generation of false signals.

Acknowledgment. We would like to thank Roche for the gift of biotinylated thiol reagents and the Commission of the European Communities, Project TRACEBACK (FP6-2005-FOOD-036300) for the financial support. We thank Dr. Ulrich Schlecht (Caesar Research Center, Germany) and Dr. Peter Thiesen (Nanofilm, Germany) for helpful assistance with SAW equipment and measurements. O.A. acknowledges financial support from the Max Planck Society (Germany), the Alexander von Humboldt Stiftung (Germany), and the Centro Interdisciplinario de Nanociencia y Nanotecnología (CINN) (PAE, ANPCyT, Argentina) M.Á. thanks Junta de Comunidades de Castilla la Mancha for a postdoctoral fellowship.

LA802228E